Simulation of asymmetric solar wind electron distributions

Chang-Mo Ryu,[1,a)] Hee-Chul Ahn,[1] Tongnyeol Rhee,[1] P. H. Yoon,[2,3] L. F. Ziebell,[4] R. Gaelzer,[5] and A. F. Viñas[6]
[1]*Department of Physics, POSTECH, Pohang, South Korea*
[2]*Massachusetts Technological Laboratory, Inc., 330 Pleasant Street, Belmont, Massachusetts 02478, USA*
[3]*IPST, University of Maryland, College Park, Maryland 20742, USA*
[4]*Instituto de Física, UFRGS, Porto Alegre, Rio Grande do Sul, Brazil*
[5]*Instituto de Física e Matemática, UFPel, Pelotas, Rio Grande do Sul, Brazil*
[6]*NASA Goddard Space Flight Center, Greenbelt, Maryland 20771, USA*

(Received 20 October 2008; accepted 29 January 2009; published online 4 June 2009)

The electron distributions detected in the solar wind feature varying degrees of anisotropic high-energy tail. In a recent work the present authors numerically solved the one-dimensional electrostatic weak turbulence equations by assuming that the solar wind electrons are initially composed of thermal core plus field-aligned counterstreaming beams, and demonstrated that a wide variety of asymmetric energetic tail distribution may result. In the present paper, the essential findings in this work are tested by means of full particle-in-cell simulation technique. It is found that the previous results are largely confirmed, thus providing evidence that the paradigm of local electron acceleration to high-energy tail by self-consistently excited Langmuir turbulence may be relevant to the solar wind environment under certain circumstances. However, some discrepancies are found such that the nearly one-sided energetic tail reported in the numerical solution of the weak turbulence kinetic equation is not shown. © *2009 American Institute of Physics*.
[DOI: 10.1063/1.3085795]

I. INTRODUCTION

The electron velocity distributions detected in the solar wind deviate considerably from a Maxwellian (Gaussian) distribution at the so-called high-energy tail.[1–9] Such a feature is typically described as thermal (that is, Maxwellian) core plus superthermal halo (or tail) populations. Sometimes there is a third component besides the isotropic halo—a highly anisotropic field-aligned energetic component called the Strahl.

There exists a substantial body of literature in which the origin of the core-halo electrons is discussed within the context of the Coulomb collisional dynamics combined with nonlocality.[10–19] Coulomb collisions in plasmas can be modeled by Landau or Balescu–Lenard equations, and such an approach is valid when collective fluctuations (i.e., instabilities) in plasmas are negligible. In this approach, the dependence of the Coulomb collisionality on the distance away from the Sun is taken into account. Near the Sun, the plasma is highly collisional, while in the corona and interplanetary space collisions are extremely rare. Thus, nonlocal evolution of the electron distribution along the diverging magnetic field and decreasing ambient density account for the observed energetic tail population.

While the global Coulomb collisional dynamics may satisfactorily account for the observed solar electron distribution in an overall sense, under certain circumstances, electrons may undergo local acceleration by self-consistently generated turbulence. This may happen if there exists a source of instability such as field-aligned electron beams. Even for quasisteady state solar wind, there will always be some temporal variations associated with the solar wind output. As the solar wind expands into the surrounding interplanetary medium, the faster electrons outpacing the slow ones will inevitably lead to the formation of the field-aligned beams. Of course, the beam formation will be much more pronounced for transient events such as the flares, but even the quiet solar wind will nevertheless have a certain degree of transient behavior such that the assumption of the existence of the field-aligned beam is not unreasonable.

The Langmuir wave excited by electron beam-plasma instability is a textbook problem. However, it is not so widely known that the Langmuir turbulence leads to the acceleration of electrons to high-velocity regime in the nonlinear phase, thus forming the non-Gaussian tail component. Such a wave-particle resonant acceleration concept[20–22] is intimately related to the second-order (or statistical) Fermi acceleration theory. In most of the wave-acceleration theory, the wave spectra are simply assumed to be given and the electron quasilinear diffusion equation is solved—that is, such a method is non-self-consistent.[23–28] More complete self-consistent treatments of the problem within the context of Langmuir turbulence include heuristic theory based upon Zakharov-type strong turbulence concept[29–31] and self-consistent weak turbulence method.[32–34]

Typical core-halo electron distributions measured in the solar wind are often modeled by the kappa distributions.[10,11,35] Often, however, they feature highly asymmetric tails such that a single kappa fit is not possible. In a recent paper[36] we have proposed a potential explanation for the asymmetry by assuming two tenuous electron beams counterstreaming with respect to each other. Numerical solutions of self-consistent weak turbulence equations showed that a

[a)]Electronic mail: ryu201@postech.ac.kr.

 © 2009 American Institute of Physics

Downloaded 08 Mar 2011 to 128.183.169.235. Redistribution subject to AIP license or copyright; see http://pop.aip.org/about/rights_and_permissions

wide variety of asymmetric superthermal tails can be formed as a result of turbulence acceleration. The key difference between Ref. 36 and similar earlier works[32–34] is that this work assumed two counterstreaming electron beams while Refs. 32–34 assumed a single beam.

At 1 a.u., the interplanetary magnetic field structure may be rather complicated, but when both foot points of the field line loops are located on the Sun, then the field-aligned motion of the electrons may be characterized as counterstreaming. Sunward-propagating beams may also be observed inside closed magnetic field structures, which can be generated by flare-induced interplanetary shock waves.[5] In such situations, the assumption of counterstreaming population is justifiable, and with the counterstreaming electron beams, Ref. 36 showed that asymmetric energetic tail population could be generated in a coupled set of wave kinetic and particle kinetic equations. The purpose of the present article is to further verify the counterstreaming beam-induced asymmetric superthermal tail generation process by means of one-dimensional (1D) electrostatic (ES) fully nonlinear particle-in-cell (PIC) simulation technique.

II. PIC SIMULATION

In the present work, we employ 1D ES PIC simulation code with a periodic boundary condition. The number of grids employed in the run is 8.4×10^6, and 80 electrons and ions were initially allocated per each cell. Consequently the total number of plasma particles reaches 6.7×10^8. In order to simulate the formation of superthermal tail distribution, one needs a sufficiently large number of particles since the number density associated with the superthermal population is many orders of magnitude lower than the bulk population. The grid size in our simulation is normalized such that $\Delta x=1$ always, which is proportional to the Debye length. The time scale is normalized by $1/(8\omega_{pe})$ such that the simulated electron plasma frequency ω_{pe} is fixed at 0.125. The simulation is normally run up to 32 768 time steps with $\Delta t=2$.

Many excellent PIC simulations of weak beam-plasma interaction problems have been performed in the past.[37–41] However, previous PIC simulations did not succeed in clearly demonstrating the generation of superthermal tail population by turbulence until recently.[42] It is also important to note that Vlasov simulation cannot produce superthermal population because of the lack of a proper dissipation mechanism.[42]

We consider two cases. First is a single component, forward-propagating electron beam with 1% density when compared to the background electron density (in this case, we designate the ratio of forward beam to background density as $n_f=0.01$). In the second situation, we simulate counterstreaming electron beams, each with 1% density ratio with respect to the background ($n_b=0.01=n_f$). The absolute value of the beam drift speed is always four times the background thermal speed. Thus, in the case of a single beam, the normalized drift speed is $U_f=4$, and for counterstreaming case, the magnitudes of two drift velocities are $U_f=4$ and $U_b=-4$, respectively. Important input physical parameters are the ratios of the forward and backward-propagating electron beam densities to the background number density, n_f and n_b, and the ratios of forward and backward beam drift speeds to the thermal speed, U_f and U_b. The choice of physical parameters is according to the papers by Gaelzer *et al.*[36] and by Nieves-Chinchilla and Viñas.[43]

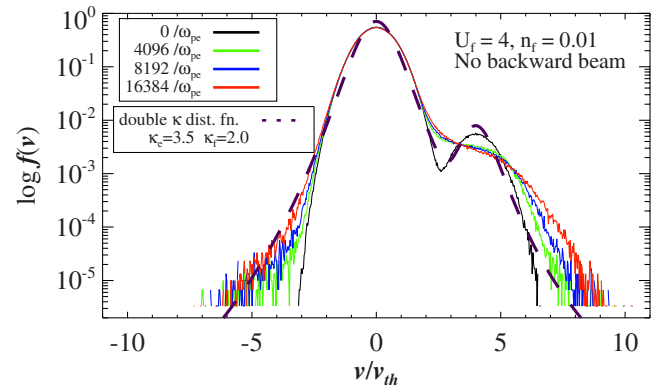

FIG. 1. (Color online) Asymmetric electron distribution function simulated using a single component of the electron beam population initially drifting in the background plasma.

Since the numerical heating rate decreases with the increase in the Debye length as $(\Delta x/\lambda_D)^3$, we have chosen the Debye length to be $5\sim10\Delta x$ in order to reduce the numerical heating induced by finite grids. The ion temperature is chosen to be 1/3 of the electron temperature. Normalization of each physical quantity is taken such that the velocity is normalized with respect to the (Maxwellian) thermal speed, $v\rightarrow v/v_e$ (where $v_e=\sqrt{2T/m}$, T being the background electron temperature and m being the electron mass), the wave number is normalized according to $k\rightarrow kv_e/\omega_p$ (where $\omega_p=\sqrt{4\pi ne^2/m}$ is the plasma frequency), and time is normalized with respect to the inverse plasma frequency, $t\rightarrow\omega_p t$. Both the particle and wave energies are normalized with respect to the electron thermal energy. The ion-to-electron mass ratio is chosen as a realistic one, $m_i/m_e=1836$.

Figure 1 displays an asymmetric tail distribution in which a single component forward-propagating electron beam characterized by $U_f=4$ and $n_f=0.01$ is considered initially. The velocity spread (i.e., the beam temperature) is the same as the ambient electron temperature. The distribution function is shown at $0\omega_{pe}^{-1}$ (initial configuration), $4096\omega_{pe}^{-1}$, $8192\omega_{pe}^{-1}$, and at $16384\omega_{pe}^{-1}$. The simulated electron distribution features overall morphology that is rather reminiscent of the typical asymmetric solar wind electron distribution (for instance, see the example in Ref. 36). The simulated distribution is also consistent with the numerical solution presented in Refs. 36 and 42. The energetic tail population (those electrons with velocity exceeding the original beam energy) can be seen to be enhanced as time progresses. The long non-Gaussian tail is reminiscent of the kappa distribution, but in order to fit the simulated distribution, one has to use two different kappa models for positive and negative portions of the velocity space. The dashed line in Fig. 1

Downloaded 08 Mar 2011 to 128.183.169.235. Redistribution subject to AIP license or copyright; see http://pop.aip.org/about/rights_and_permissions

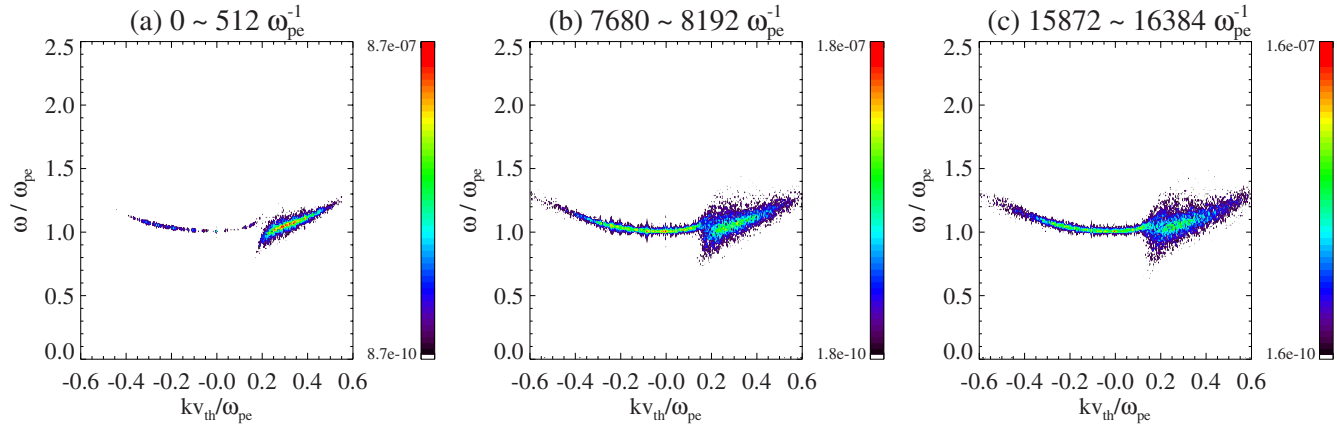

FIG. 2. (Color online) Frequency-wave number spectra at three different time intervals during which asymmetric electron distribution function shown in Fig. 1 is formed.

depicts the double kappa distribution function defined below, with $\kappa_e=3.5$ for the background electrons and $\kappa_f=2.0$ for the forward beam electron, respectively,

$$f(v) = \frac{n_e}{\pi^{1/2} v_e} \frac{\Gamma(\kappa_e+1)}{\kappa_e^{1/2}\Gamma(\kappa_e+1/2)} \frac{1}{(1+v^2/\kappa_e v_e^2)^{\kappa_e+1}} + \frac{n_f}{\pi^{1/2} v_f} \frac{\Gamma(\kappa_f+1)}{\kappa_f^{1/2}\Gamma(\kappa_f+1/2)} \frac{1}{(1+(v-U_f)^2/\kappa_f v_f^2)^{\kappa_f+1}}. \tag{1}$$

Here, $v_{e,f}$ are Maxwellian thermal speeds associated with the background electrons and forward beam electrons. For kappa distributions it is well known that the effective temperature $T_{e,f}^{\text{kappa}}$ is not the same as the Maxwellian counterpart. As a matter of fact, the effective temperature for kappa model is enhanced over Maxwellian temperature $T_{e,f}^{\max}=mv_{e,f}^2/2$ by

$$T_{e,f}^{\text{kappa}} = T_{e,f}^{\max} \frac{\kappa_{e,f}}{\kappa_{e,f}-1/2}.$$

Figure 2 displays a series of wave spectra averaged over time intervals beginning at $0\omega_{pe}^{-1}$ until the next time step, $4096\omega_{pe}^{-1}$, then averaged from the time step $4096\omega_{pe}^{-1}$ to $8192\omega_{pe}^{-1}$, and finally from $8192\omega_{pe}^{-1}$ to $16\,384\omega_{pe}^{-1}$. As Fig. 2 shows, the enhancement of the ES fluctuation can be clearly discerned in the vicinity of the Langmuir wave dispersion relation, $\omega^2=\omega_p^2+3k^2v_{\text{th}}^2/4$. It is noteworthy that forward-propagating waves (i.e., positive k space) are particularly enhanced. This is the primary Langmuir wave excited by linear wave-particle resonance and the positive slope associated with the beam. However, it should be noted that the primary Langmuir waves are not directly responsible for the generation of the superthermal tail, but rather it is the long-wavelength (small k) Langmuir condensate modes that are in resonance with the electrons in the non-Gaussian tail region.

In contrast to Fig. 1 which shows electron distribution with asymmetric non-Gaussian superthermal tails on either side of the positive and negative v space, Fig. 3 shows a symmetric pair of non-Gaussian tails. In order to generate this result, we have initiated the simulation with a pair of counterstreaming electron beams characterized by $U_f=4$, $n_f=0.01$, $U_b=-4$, and $n_b=0.01$. Simulated distribution functions are plotted at $0\omega_{pe}^{-1}$, $4096\omega_{pe}^{-1}$, $8192\omega_{pe}^{-1}$, and $16\,384\omega_{pe}^{-1}$ using different color codes, as before. Again, the simulation results are in overall agreement with the numerical solution of weak turbulence equation by Gaelzer *et al.*[36]

Finally, in Fig. 4 we show the frequency-wave number spectra (the numerical dispersion relation) corresponding to the asymmetric tail distribution shown in Fig. 3. The time intervals are the same as described in Fig. 2. As expected, enhanced Langmuir waves generated by both the forward- and backward-propagating electron beams feature an inversion symmetry $k\leftrightarrow -k$. As with the asymmetric case, however, it is not the broad range of linearly unstable Langmuir wave excitation that leads to the generation of the energetic tails (these only lead to the plateau formation), but it is the long-wavelength (small k) spectra sandwiched between the two wings that are in resonance with the energetic particles in the tail. The generation of the long-wavelength, small k Langmuir waves is the direct consequence of nonlinear wave-wave and nonlinear wave-particle interactions.

The simulation results discussed thus far are in overall agreement with our earlier paper.[36] However, we also found some discrepancies. In Ref. 36, it was reported that under certain circumstances the asymmetry on the energetic tail can be greatly enhanced. In general, if the magnitude and the densities of the counterstreaming beams were equal as in our

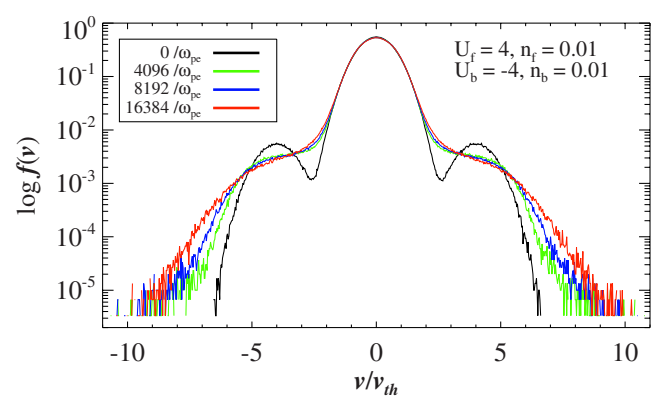

FIG. 3. (Color online) Symmetric electron distribution function simulated with initially counterstreaming beams immersed in the background plasma.

Downloaded 08 Mar 2011 to 128.183.169.235. Redistribution subject to AIP license or copyright; see http://pop.aip.org/about/rights_and_permissions

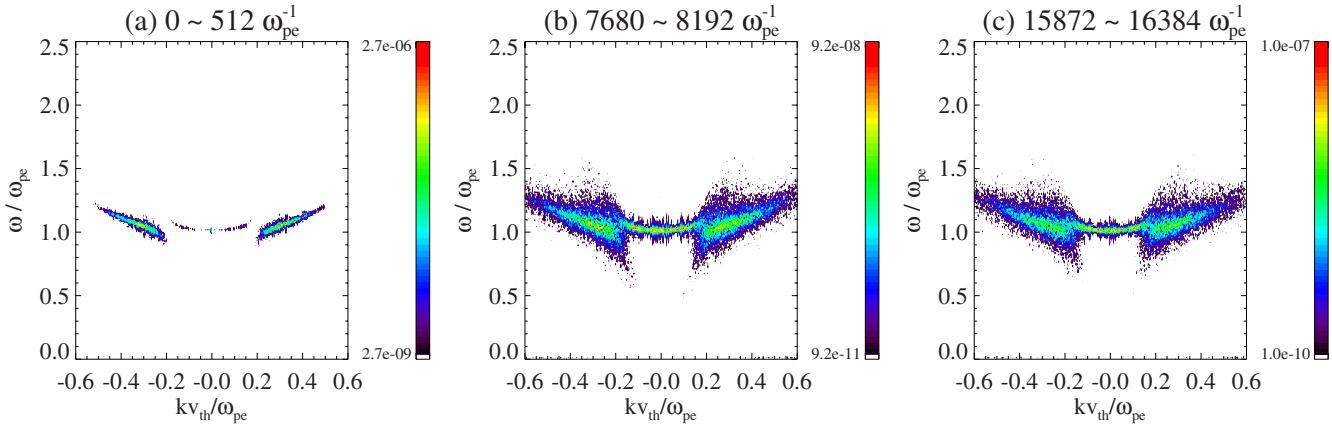

FIG. 4. (Color online) Frequency-wave number dispersion relation spectra at three different time interval during which symmetric electron distribution function shown in Fig. 3 was generated.

Figs. 3 and 4, then indeed, the electron distribution featured symmetry, as we also find in this paper. In Ref. 36 we found that when there is only a single beam, then there is an inherent asymmetry associated with the energetic tail (which is consistent with Figs. 1 and 2). However, Ref. 36 also reported an intriguing case in which, when the counterstreaming beams do not possess exactly matching magnitudes of the drift speed, then one side of the tail distribution can become greatly enhanced while the tail formation on the opposite side is suppressed. Thus far, however, according to our simulation study, we were not able to confirm such a finding. According to our simulation, we have only been able to confirm a linear relationship between the degree of anisotropy and the magnitude of the backward-streaming beam drift velocity or the density. However, we could still demonstrate in PIC simulation that it is possible to generate a varying degree of asymmetric electron distribution function by positing the presence of a secondary backward-drifting electron component. We believe that this result may be relevant to the observed solar wind electron distributions, under certain circumstances.

III. CONCLUSIONS AND DISCUSSION

The electron distributions detected in the solar wind feature varying degrees of anisotropic high-energy tail. In a recent work,[36] 1D ES weak turbulence equations are numerically solved by assuming that the solar wind electrons are initially composed of thermal core plus field-aligned counterstreaming beams. The justification for such counterstreaming beams is that even for quasisteady state solar wind, there will always be some temporal variations associated with the solar wind output such that the formation of the field-aligned beams may be possible. If both foot points of the interplanetary magnetic field line loops at 1 a.u. are anchored on the Sun, then a counterstreaming beam may also be present along the field line. Under such an assumption, we demonstrated that a wide variety of asymmetric energetic tail distribution may result depending on the relative magnitude of the counterstreaming beam drift speeds and the relative densities.

In the present paper, the major findings in Ref. 36 obtained by solving weak turbulence equation are examined by employing a full PIC simulation technique. It is found that the results obtained from solving theoretical equations are largely confirmed in that, for counterstreaming beams with equal magnitude and density, the resulting electron distribution features highly symmetric energetic tail, while for a single beam, the final distribution features an asymmetric tail. However, we also found some discrepancies. In particular, whereas Ref. 36 reported highly one-sided tail distribution when the forward and backward beam speeds happen to be at a certain critical value, we found no such behavior in the simulation. However, the essential paradigm of electron acceleration to high-energy tail population by self-consistently excited Langmuir turbulence is still intact. In short, the findings in the previous paper[36] and the present paper may be relevant to the interpretation of the asymmetric electron population data obtained in the solar wind environment near 1 a.u.

Before we close, we note that the observed solar wind electron distributions may represent an alternative statistical mechanical equilibrium known as nonextensive thermodynamical equilibrium state.[44] The nonextensive thermostatistics is appropriate for statistical systems interacting through long-range forces. Tsallis' general work was further elaborated by Treumann.[45,46] One of the consequences of this new idea is that the (single or multiple) kappa distribution is a natural equilibrium state of the nonextensive statistics, just as the Maxwellian or Gaussian distribution is the equilibrium solution of the customary Boltzmann (or extensive) statistics.[47–50] In spite of this, the problem of dynamical accessibility of the kappa distribution from an arbitrary initial state has not been adequately addressed so far. The present paper may be important in this regard, namely, we have shown that an initial distribution of a core Gaussian distribution of plasma and a pair of counterstreaming electron beams leads to the excitation of Langmuir turbulence, but in an asymptotic state, the system reaches a quasisteady state that is best modeled by a pair of kappa distributions.

Downloaded 08 Mar 2011 to 128.183.169.235. Redistribution subject to AIP license or copyright; see http://pop.aip.org/about/rights_and_permissions

ACKNOWLEDGMENTS

This work was supported by Grant No. R11-2008-072-01003-0 of the Korea Science and Engineering Foundation and StSc program by POSCO. Numerical computations were performed with the support from KISTI under the 6th Strategic Supercomputing Applications Support Program. C.M.R. acknowledges the technical support from S. M. Lee of the Supercomputing Center. This work has been partially supported by the Brazilian agencies Conselho Nacional de Desenvolvimento Científico e Tecnológico (CNPq) and Fundação de Amparo à Pesquisa do Estado do Rio Grande do Sul (FAPERGS). The research by P.H.Y. was supported by AFOSR under Contract No. FA9550-07-0053.

[1] W. C. Feldman, J. R. Asbridge, S. J. Bame, M. D. Montgomery, and S. P. Gary, J. Geophys. Res. **80**, 4181, DOI:10.1029/JA080i031p04181 (1975).
[2] R. P. Lin, D. W. Potter, D. A. Gurnett, and F. L. Scarf, Astrophys. J. **251**, 364 (1981).
[3] R. P. Lin, W. K. Levedahl, W. Lotko, D. A. Gurnett, and F. L. Scarf, Astrophys. J. **308**, 954 (1986).
[4] W. G. Pilipp, H. Miggennieder, M. S. Montgomery, K.-H. Mühläuser, H. Rosenbauer, and R. Schwenn, J. Geophys. Res. **92**, 1075, DOI:10.1029/JA092iA02p01075 (1987).
[5] W. G. Pilipp, H. Miggennieder, M. S. Montgomery, K.-H. Mühläuser, H. Rosenbauer, and R. Schwenn, J. Geophys. Res. **92**, 1093 (1987).
[6] S. P. Christon, D. G. Mitchell, D. J. Williams, L. A. Frank, C. Y. Huang, and T. E. Eastman, J. Geophys. Res. **93**, 2562 (1988).
[7] R. J. Fitzenreiter, J. D. Scudder, and A. J. Klimas, J. Geophys. Res. **95**, 4155, DOI:10.1029/JA095iA04p04155 (1990).
[8] R. J. Fitzenreiter, K. W. Ogilvie, D. J. Chornay, and J. Keller, Geophys. Res. Lett. **25**, 249, DOI:10.1029/97GL03703 (1998).
[9] R. E. Ergun, D. Larson, R. P. Lin, J. P. McFadden, C. W. Carlson, K. A. Anderson, L. Muschietti, M. McCarthy, G. K. Parks, H. Reme, J. M. Bosqued, C. D'Uston, T. R. Sanderson, K. P. Wenzel, S. D. Bale, P. Kellogg, and J.-L. Bougeret, Astrophys. J. **503**, 435 (1998).
[10] J. D. Scudder and S. Olbert, J. Geophys. Res. **84**, 2755, DOI:10.1029/JA084iA06p02755(1979).
[11] J. D. Scudder and S. Olbert, J. Geophys. Res. **84**, 6603, DOI:10.1029/JA084iA11p06603 (1979).
[12] E. Marsch and S. Livi, Phys. Fluids **28**, 1379 (1985).
[13] M. V. Canullo, A. Costa, and C. F. Fontáin, Astrophys. J. **462**, 1005 (1996).
[14] Ø. Lie-Svendsen, V. H. Hansteen, and F. Leer, J. Geophys. Res. **102**, 4701, DOI:10.1029/96JA03632 (1997).
[15] V. Pierrard, M. Maksimovic, and J. Lemaire, J. Geophys. Res. **104**, 17021, DOI:10.1029/1999JA900169 (1999).
[16] V. Pierrard, M. Maksimovic, and J. Lemaire, Astrophys. Space Sci. **277**, 195 (2001).
[17] V. Pierrard, M. Maksimovic, and J. Lemaire, J. Geophys. Res. **106**, 29305, DOI:10.1029/2001JA900133 (2001).
[18] S. Landi and F. G. E. Pantellini, Astron. Astrophys. **372**, 686 (2001).
[19] J. C. Dorelli and J. D. Scudder, J. Geophys. Res. **108**, 1294, DOI:10.1029/2002JA009484 (2003).
[20] A. V. Gurevich, Sov. Phys. JETP **11**, 1150 (1960).
[21] B. A. Tverskoi, Sov. Phys. JETP **26**, 821 (1968).
[22] S. B. Pikel'ner and V. N. Tsytovich, Sov. Phys. JETP **28**, 507 (1969).
[23] A. Hasegawa, K. Mima, and M. Duong-van, Phys. Rev. Lett. **54**, 2608 (1985).
[24] C.-Y. Ma and D. Summers, Geophys. Res. Lett. **25**, 4099, DOI:10.1029/1998GL900108 (1998).
[25] D. A. Roberts and J. A. Miller, Geophys. Res. Lett. **25**, 607, DOI:10.1029/98GL00328 (1998).
[26] M. P. Leubner, Planet. Space Sci. **48**, 133 (2000).
[27] C. Vocks and G. Mann, Astrophys. J. **593**, 1134 (2003).
[28] C. Vocks, C. Salem, R. P. Lin, and G. Mann, Astrophys. J. **627**, 540 (2005).
[29] V. V. Gorev, A. S. Kingsep, and V. V. Yan'kov, Sov. Phys. JETP **43**, 479 (1976).
[30] A. S. Kingsep, Sov. Phys. JETP **47**, 51 (1978).
[31] G. Pelletier, Phys. Rev. Lett. **49**, 782 (1982).
[32] P. H. Yoon, T. Rhee, and C.-M. Ryu, Phys. Rev. Lett. **95**, 215003 (2005).
[33] P. H. Yoon, T. Rhee, and C.-M. Ryu, J. Geophys. Res. **111**, A09106 (2006).
[34] T. Rhee, C.-M. Ryu, and P. H. Yoon, J. Geophys. Res. **111**, A09107 (2006).
[35] V. M. Vasyliunas, J. Geophys. Res. **73**, 2839 (1968).
[36] R. Gaelzer, and L. F. Ziebell, A. F. Viñas, P. H. Yoon, and C.-M. Ryu, Astrophys. J. **677**, 676 (2008).
[37] J. M. Dawson and R. Shanny, Phys. Fluids **11**, 1506 (1968).
[38] R. L. Morse and C. W. Nielson, Phys. Fluids **12**, 2418 (1969).
[39] P. L. Pritchett and J. M. Dawson, Phys. Fluids **26**, 1114 (1983).
[40] I. H. Cairns and K.-I. Nishikawa, J. Geophys. Res. **94**, 79 (1989).
[41] C. T. Dum, J. Geophys. Res. **95**, 8095 (1990); **95**, 8111 (1990); **95**, 8123 (1990).
[42] C.-M. Ryu, T. Rhee, T. Umeda, P. H. Yoon, and Y. Omura, Phys. Plasmas **14**, 100701 (2007).
[43] T. Nieves-Chinchilla and A. F. Viñas, J. Geophys. Res. **113**, A02105, DOI:10.1029/2007JA012703 (2008).
[44] C. Tsallis, J. Stat. Phys. **52**, 479 (1988).
[45] R. A. Treumann, Phys. Scr. **59**, 19 (1999).
[46] R. A. Treumann, Phys. Scr. **59**, 204 (1999).
[47] M. P. Leubner, Astrophys. Space Sci. **282**, 573 (2002).
[48] M. P. Leubner, Astrophys. J. **604**, 469 (2004).
[49] M. P. Leubner, Phys. Plasmas **11**, 1308 (2004).
[50] M. P. Leubner and Z. Vörös, Nonlinear Processes Geophys. **12**, 171 (2005).

Downloaded 08 Mar 2011 to 128.183.169.235. Redistribution subject to AIP license or copyright; see http://pop.aip.org/about/rights_and_permissions